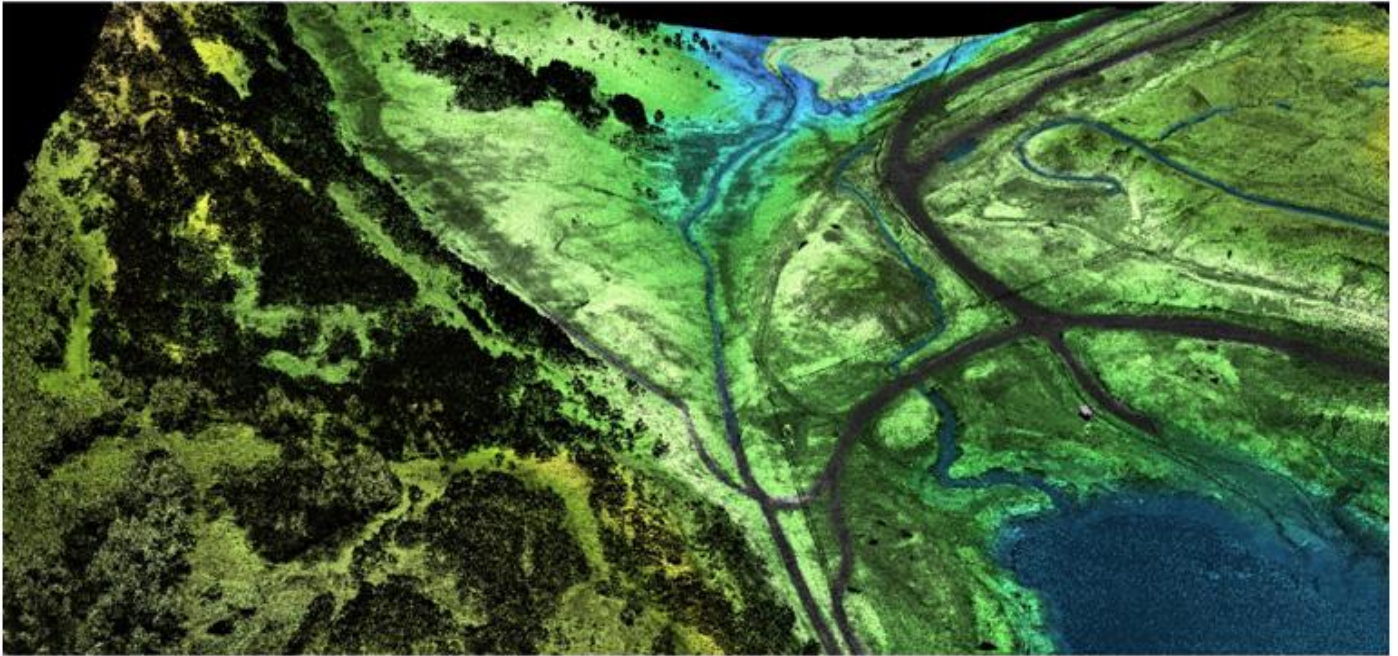


# LiDAR REMOTE SENSING


## CHEHALIS RIVER WATERSHED • WASHINGTON

August 20, 2012



**PUGET SOUND LiDAR CONSORTIUM**

DIANA MARTINEZ - 1011 Western Ave., Suite 500 - Seattle, WA 98104

 **WATERSHED SCIENCES** • 517 SW 2nd Street, Suite 400 - Corvallis, OR 97333



# LIDAR REMOTE SENSING DATA COLLECTION: CHEHALIS RIVER WATERSHED STUDY AREA

## TABLE OF CONTENTS

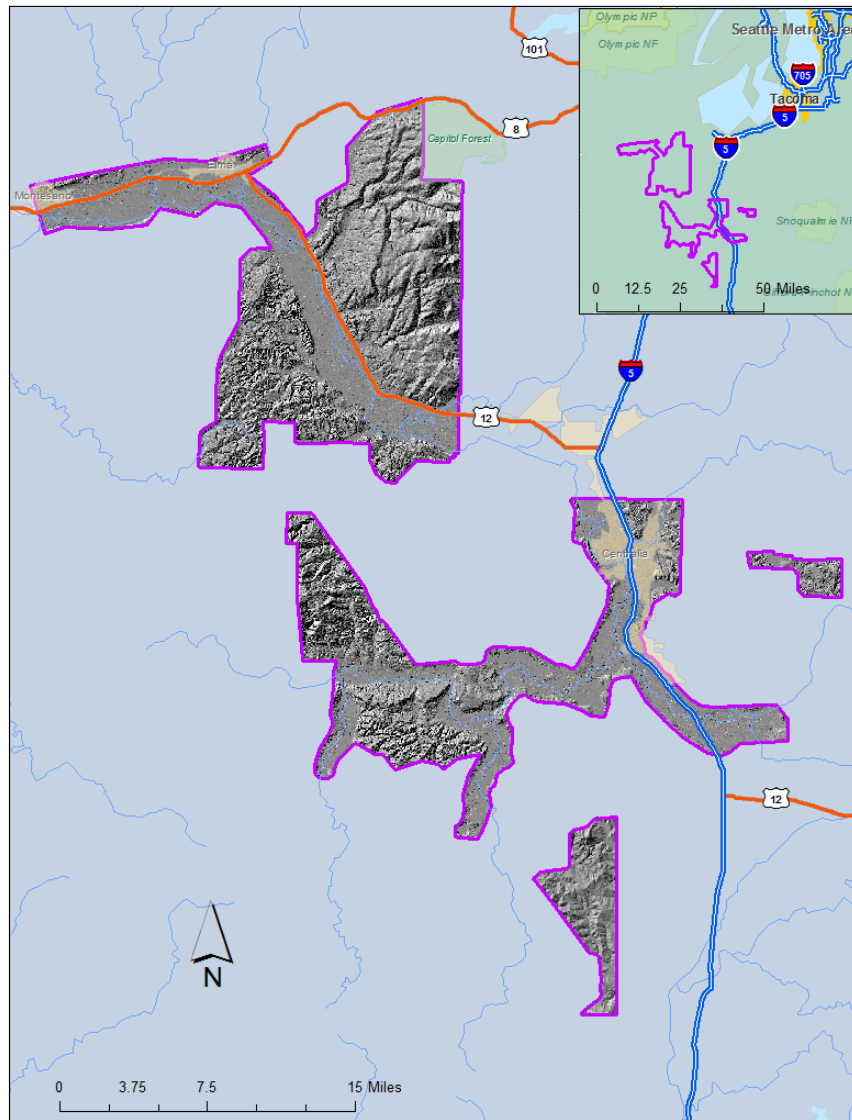
1. Overview .....	1
2. Acquisition .....	2
2.1 Airborne Survey - Instrumentation and Methods .....	2
2.2 Ground Survey - Instrumentation and Methods .....	3
2.2.1 Instrumentation .....	3
2.2.2 Monumentation .....	4
2.2.3 Methodology .....	5
2.2.4 Monument Accuracy .....	6
3. LiDAR Data Processing .....	8
3.1 Applications and Work Flow Overview .....	8
3.3 Laser Point Processing .....	9
4. LiDAR Accuracy Assessment .....	10
4.1 Laser Noise and Relative Accuracy .....	10
4.2 Absolute Accuracy .....	11
5. Study Area Results .....	11
5.1 Data Summary .....	11
5.2 Data Density/Resolution .....	12
5.3 Relative Accuracy Calibration Results .....	16
5.4 Absolute Accuracy .....	17
5.5 Land Cover Accuracy .....	18
6. Temporal Variations .....	19
7. Hydro Flattened Models .....	20
8. Projection/Datum and Units .....	22
9. Deliverables .....	22
10. Certifications .....	24
11. Selected Images .....	25
12. Glossary .....	28
13. Citations .....	29
Appendix A .....	30



# 1. Overview

Watershed Sciences, Inc. (WSI) collected Light Detection and Ranging (LiDAR) data for the Chehalis River Watershed study area on January 28<sup>th</sup>, February 2<sup>nd</sup>-7<sup>th</sup>, March 4<sup>th</sup>-9<sup>th</sup>, March 21<sup>st</sup>-23<sup>rd</sup>, and April 7<sup>th</sup>, 2012 for the Puget Sound LiDAR Consortium in partnership with the Federal Emergency Management Agency Region X (FEMA), Washington Department of Natural Resources, and Lewis County. This report documents the data acquisition, processing methods, accuracy assessment, and deliverables for the Chehalis River Watershed area of interest (AOI) in Washington State. The requested area of 224,713 acres for the Chehalis River Watershed was expanded to include a 100m buffer to ensure complete coverage and adequate point densities around survey area boundaries resulting in a total of 234,556 acres of delivered LiDAR data.

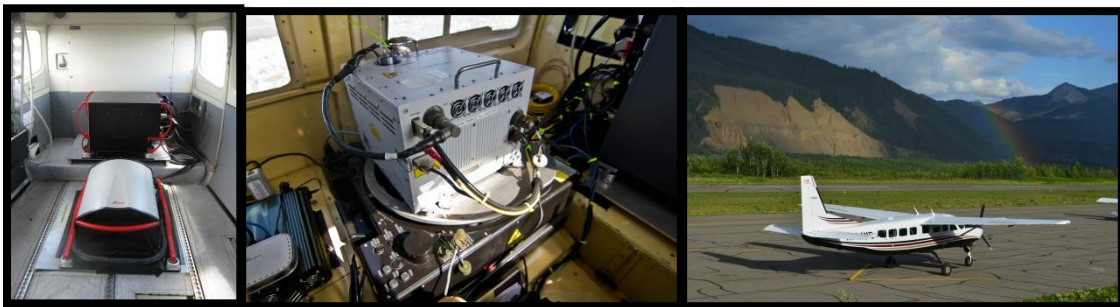
*Figure 1. Chehalis River Watershed area of interest, Washington.*



## 2.Acquisition

### 2.1 Airborne Survey - Instrumentation and Methods

The LiDAR survey utilized an Optech Orion-C and a Leica ALS60 sensor in a Cessna Caravan 208B. Depending on acquisition day weather and terrain, the Leica system was set to acquire from  $\geq 83,000$  to 105,000 laser pulses per second (i.e., 83 - 105.0 kHz pulse rate) and flown at 900-1300 meters above ground level (AGL), capturing a scan angle of  $\pm 14^\circ$  from nadir. The Optech System was set to acquire from  $\geq 83,000$  to 100,000 laser pulses per second (i.e., 83-100.0 kHz pulse rate) and flown at 800-1000 meters AGL, capturing a scan angle of  $\pm 14^\circ$  from nadir. These settings were developed to yield points with an average native pulse density of  $\geq 8$  pulses per square meter over terrestrial surfaces. It is not uncommon for some types of surfaces (e.g. dense vegetation or water) to return fewer pulses than the laser originally emitted. These discrepancies between 'native' and 'delivered' density will vary depending on terrain, land cover, and the prevalence of water bodies.



*The Cessna Caravan is a stable platform, ideal for flying slow and low for high density projects. The Leica ALS60 sensor head installed in the Caravan is shown on the left. The Orion sensor head is shown in the middle. The caravan we use for data acquisition is shown on the right.*

For each flight, steps are taken to initialize and calibrate the sensor. Prior to take off a static initialization is completed on the ground. After the sensor has been turned on, the plane sits in an area unobstructed by buildings, for 3 minutes to establish a quality Global Positioning System (GPS) solution. When the aircraft is within 10nm of base stations an S-Turn (90 degrees out, 180 back and 90 to get back on line) is completed to make sure the sensor IMU is initialized. At the end of the mission, over or near the study area, a complete figure-eight is flown.

The entire area was surveyed with an opposing flight line side-lap of  $\geq 60\%$  ( $\geq 100\%$  overlap) to reduce laser shadowing and increase surface laser painting. The Leica and Optech laser systems allow up to four range measurements (returns) per pulse, and all discernible laser returns were processed for the output dataset.

To accurately solve for laser point position (geographic coordinates x, y, z), the positional coordinates of the airborne sensor and the attitude of the aircraft were recorded continuously throughout the LiDAR data collection mission. Aircraft position was measured twice per second (2 Hz) by an onboard differential GPS unit. Aircraft attitude was measured 200 times per second (200 Hz) as pitch, roll and yaw (heading) from an onboard inertial measurement

unit (IMU). To allow for post-processing correction and calibration, aircraft/sensor position and attitude data are indexed by GPS time.

Upon completion of each flight the data was backed up and then reviewed by the operator. This review is performed on raw flight data in the field using IPAS Pro, ALS LiDAR Point Processor, ArcMap, Microstation, and Corpscon software. It is a cursory inspection to test for full coverage along the flight lines. This review process ensures the consistency of the laser settings and timestamps as well as converts the data to images that can be visually inspected for data gaps so reflies can be completed as necessary.

## 2.2 Ground Survey - Instrumentation and Methods



During the LiDAR survey, static (1 Hz recording frequency) ground surveys were conducted over set monuments. Monument coordinates are provided in Table 1 and shown in Figure 2 for the AOI. After the airborne survey, the static GPS data were processed using triangulation with Continuously Operating Reference Stations (CORS) and checked using the Online Positioning User Service (OPUS<sup>1</sup>) to quantify daily variance. Multiple sessions were processed over the same monument to confirm antenna height measurements and reported position accuracy. Indexed by time, these GPS data were used to correct the continuous

onboard measurements of aircraft position recorded throughout the mission. Control monuments were located within 13 nautical miles of the survey area.

### 2.2.1 Instrumentation

For this study area all Global Navigation Satellite System survey work utilized a Trimble GPS receiver model R7 GNSS with a Zephyr Geodetic Model 2 RoHS antenna with ground plane (OPUS ID: TRM57971.00) and a Trimble model R8 GNSS unit (OPUS ID: TRM\_R8\_GNSS) for static control points. A Trimble model R8 GNSS unit was used for collecting check points using real time kinematic (RTK) survey techniques. All GPS measurements are made with dual frequency L1-L2 receivers with carrier-phase correction.

---

<sup>1</sup> Online Positioning User Service (OPUS) is run by the National Geodetic Survey to process corrected monument positions.

### 2.2.2 Monumentation



Watershed Sciences utilized one established monument and established twelve new monuments in the area. The Watershed Sciences' monumentation was implemented with 5/8" x 30" rebar topped with a metal cap stamped with the project ID and year. Monuments selected were found to have good visibility and optimal location to support a LiDAR acquisition flight.

*Table 1. Base Station control coordinates for the Chehalis River Watershed LiDAR data collection.*

Base Station ID	Datum: NAD83 (CORS96)		GRS80
	Latitude	Longitude	Ellipsoid Z (meters)
CH_BLM	46° 49' 57.46091" N	123° 13' 59.11509" W	3.993
CH_01	46° 55' 56.01899" N	123° 19' 54.84926" W	-2.074
CH_02	46° 56' 23.02591" N	123° 20' 40.34710" W	-6.783
CH_03	46° 38' 03.90618" N	123° 15' 48.42561" W	72.190
CH_04	46° 35' 10.37819" N	123° 17' 06.32198" W	95.947
CH_05	46° 37' 35.62484" N	123° 04' 29.17506" W	39.458
CH_06	46° 34' 34.04218" N	122° 50' 44.63828" W	81.723
CH_07	46° 59' 24.92027" N	123° 25' 29.98866" W	-9.186
CH_08	46° 44' 00.78142" N	123° 00' 14.64531" W	30.105
CH_09	46° 51' 05.62124" N	123° 16' 38.82466" W	1.855
CH_11	46° 35' 32.17331" N	123° 07' 25.45125" W	49.275
CH_12	46° 33' 40.55689" N	123° 07' 46.12298" W	54.969
CH_13	46° 31' 22.49145 N	123° 07' 51.16129" W	79.396



### 2.2.3 Methodology

The aircraft was assigned a ground crew member with two Trimble R7 receivers and an R8 receiver. The ground crew vehicles are equipped with standard field survey supplies and equipment including safety materials. All control monuments were observed for a minimum of one survey session lasting no fewer than 4 hours and an additional session lasting no fewer than 2 hours. At the beginning of every session the tripod and antenna were reset, resulting in two independent instrument heights and data files. Data was collected at a rate of 1Hz using a 10 degree mask on the antenna.

The ground crew transferred the GPS data daily to the WSI Professional Land Surveyor (PLS) for oversight, Quality Assurance/Quality Control (QA/QC) review and processing. OPUS processing triangulates the monument position using 3 CORS stations resulting in a fully adjusted position. After multiple days of data were collected at each monument, accuracy and error ellipses were calculated from the OPUS reports. That information leads to a rating of the monument based on FGDC-STD-007.2-1998<sup>2</sup> at the 95% confidence level. See section 2.2.4 for the overall rating of the monuments used on this project. When a statistical stable position was found CORPSCON<sup>3</sup> 6.0.1 software was used to convert the UTM positions to geodetic positions. This geodetic position was used for processing the LiDAR data.

RTK and aircraft mounted GPS measurements were made during periods with PDOP<sup>4</sup> less than or equal to 3.0 and with at least 6 satellites in view of both a stationary reference receiver and the roving receiver. Periods of low precision during static sessions were removed during OPUS processing. RTK positions were collected on bare earth locations such as paved, gravel or stable dirt roads, and other locations where the ground is clearly visible (and is likely to remain visible) from the sky during the data acquisition and RTK measurement period(s). For RTK data collection, the surveyor holds an R8 GNSS Unit level and stationary for 5 seconds, while the unit calculates the pseudo range position from at least three epochs with the relative error under 1.5 cm horizontal and 2 cm vertical.

In order to facilitate comparisons with LiDAR measurements, RTK measurements were not taken on highly reflective surfaces such as center line stripes or lane markings on roads. RTK points were taken no closer than one meter to any nearby terrain breaks such as road edges or drop offs.



<sup>2</sup> Federal Geographic Data Committee Draft Geospatial Positioning Accuracy Standards (Part 2 table 2.1)

<sup>3</sup> U.S. Army Corps of Engineers , Army Geospatial Center Software

<sup>4</sup>PDOP: Point Dilution of Precision is a measure of satellite geometry, the smaller the number the better the geometry between the point and the satellites.

### 2.2.4 Monument Accuracy

FGDC-STD-007.2-1998<sup>5</sup> at the 95% confidence level for this project:

St Dev<sub>NE</sub>: 0.050 m

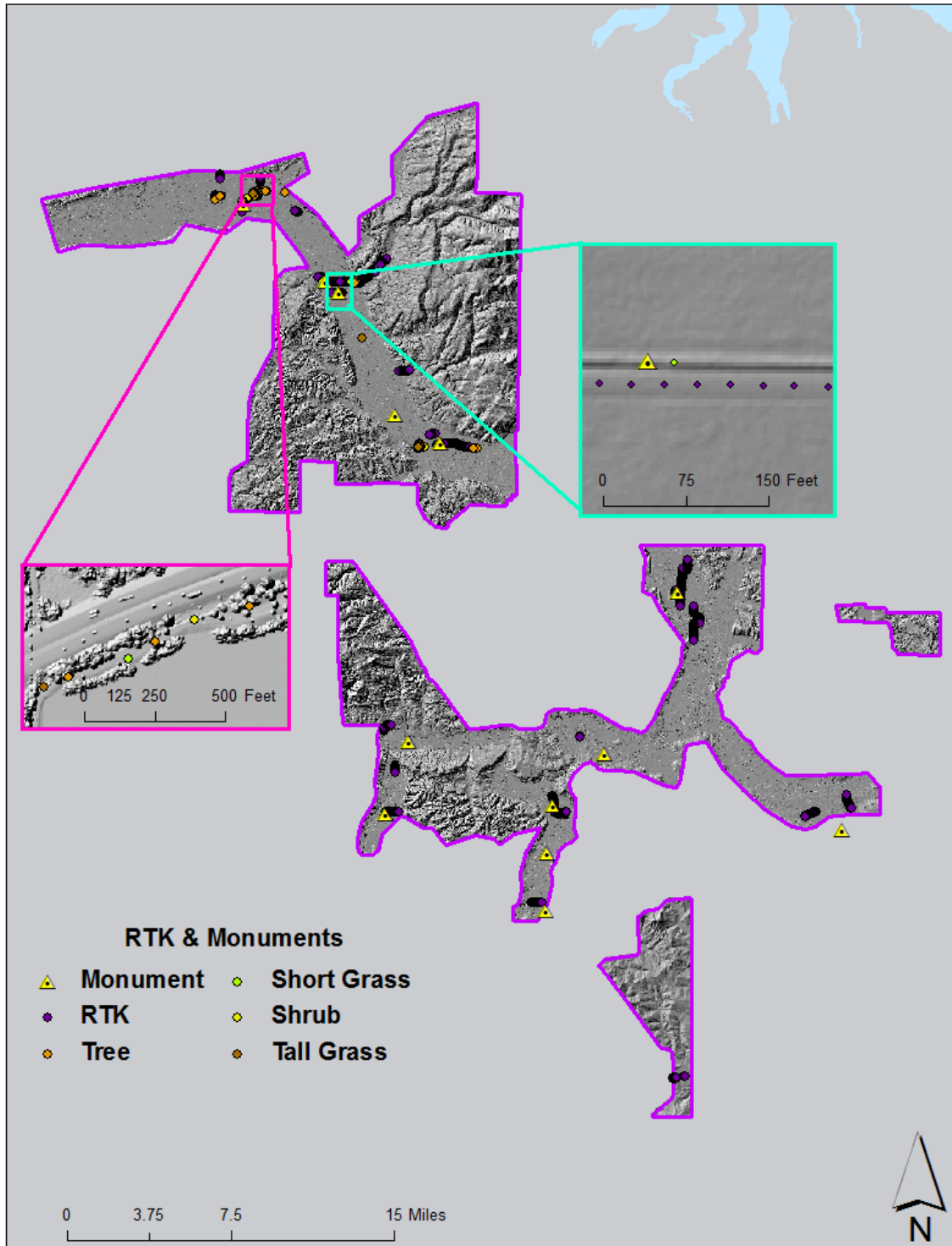
St Dev<sub>z</sub>: 0.050 m



---

<sup>5</sup> Federal Geographic Data Committee Draft Geospatial Positioning Accuracy Standards (Part 2 table 2.1)

Figure 2. RTK check point (4,331) and control monument (13) locations used in the Chehalis River Watershed AOI.



## 3. LiDAR Data Processing

### 3.1 Applications and Work Flow Overview

1. Resolved kinematic corrections for aircraft position data using kinematic aircraft GPS and static ground GPS data.  
**Software:** Waypoint GPS v.8.10, Trimble Business Center v.2.6
2. Developed a smoothed best estimate of trajectory (SBET) file that blends post-processed aircraft position with attitude data. Sensor head position and attitude were calculated throughout the survey. The SBET data were used extensively for laser point processing.  
**Software:** IPAS TC v.3.1
3. Calculated laser point position by associating SBET position to each laser point return time, scan angle, intensity, etc. Created raw laser point cloud data for the entire survey in \*.las (ASPRS v. 1.2) format. Data were then converted to orthometric elevations (NAVD88) by applying a Geoid03 correction.  
**Software:** ALS Post Processing Software v.2.74
4. Imported raw laser points into manageable blocks (less than 500 MB) to perform manual relative accuracy calibration and filter for pits/birds. Ground points were then classified for individual flight lines (to be used for relative accuracy testing and calibration).  
**Software:** TerraScan v.12.004
5. Using ground classified points per each flight line, the relative accuracy was tested. Automated line-to-line calibrations were then performed for system attitude parameters (pitch, roll, heading), mirror flex (scale) and GPS/IMU drift. Calibrations were performed on ground classified points from paired flight lines. Every flight line was used for relative accuracy calibration.  
**Software:** TerraMatch v.12.001
6. Resulting data were classified as ground and non-ground points. Statistical absolute accuracy was assessed via direct comparisons of ground classified points to ground RTK survey data.  
**Software:** TerraScan v.12.004, TerraModeler v.12.002
7. Final version of data was checked for duplicate points using TerraScan software. No duplicate points were found.  
**Software:** TerraScan v.12.004, TerraModeler v.12.002
8. Bare Earth models were created as a triangulated surface and exported as ArcInfo ASCII grids at a 3-foot pixel resolution. Highest Hit models were created for any class at 3-foot grid spacing and exported as ArcInfo ASCII grids. Hydroflattened Bare Earth models were created as a triangulated surface with breaklines enforced and exported as ArcInfo ASCII grids at a 3-foot pixel resolution.  
**Software:** TerraScan v.12.004, ArcMap v. 10.0, TerraModeler v.12.002

## 3.2 Aircraft Kinematic GPS and IMU Data

LiDAR survey datasets were referenced to the 1 Hz static ground GPS data collected over pre-surveyed monuments with known coordinates. While surveying, the aircraft collected 2 Hz kinematic GPS data, and the onboard inertial measurement unit (IMU) collected 200 Hz aircraft attitude data. Waypoint GPS v.8.10 was used to process the kinematic corrections for the aircraft. The static and kinematic GPS data were then post-processed after the survey to obtain an accurate GPS solution and aircraft positions. IPAS TC v.3.1 was used to develop a trajectory file that includes corrected aircraft position and attitude information. The trajectory data for the entire flight survey session were incorporated into a final smoothed best estimated trajectory (SBET) file that contains accurate and continuous aircraft positions and attitudes.

## 3.3 Laser Point Processing

Laser point coordinates were computed using the IPAS and ALS Post Processor software suites based on independent data from the LiDAR system (pulse time, scan angle), and aircraft trajectory data (SBET). Laser point returns (first through fourth) were assigned an associated (x, y, z) coordinate along with unique intensity values (0-255). The data were output into large LAS v. 1.2 files with each point maintaining the corresponding scan angle, return number (echo), intensity, and x, y, z (easting, northing, and elevation) information.

These initial laser point files were too large for subsequent processing. To facilitate laser point processing, bins (polygons) were created to divide the dataset into manageable sizes (< 500 MB). Flightlines and LiDAR data were then reviewed to ensure complete coverage of the survey area and positional accuracy of the laser points.

Laser point data were imported into processing bins in TerraScan, and manual calibration was performed to assess the system offsets for pitch, roll, heading and scale (mirror flex). Using a geometric relationship developed by WSI, each of these offsets was resolved and corrected if necessary.

LiDAR points were then filtered for noise, pits (artificial low points), and birds (true birds as well as erroneously high points) by screening for absolute elevation limits, isolated points and height above ground. Each bin was then manually inspected for remaining pits and birds and spurious points were removed. In a bin containing approximately 7.5-9.0 million points, an average of 50-100 points are typically found to be artificially low or high. Common sources of non-terrestrial returns are clouds, birds, vapor, haze, decks, brush piles, etc.

Internal calibration was refined using TerraMatch. Points from overlapping lines were tested for internal consistency and final adjustments were made for system misalignments (i.e., pitch, roll, heading offsets and scale). Automated sensor attitude and scale corrections yielded 3-5 cm improvements in the relative accuracy. Once system misalignments were corrected, vertical GPS drift was then resolved and removed per flight line, yielding a slight improvement (<1 cm) in relative accuracy.

The TerraScan software suite is designed specifically for classifying near-ground points (Soininen, 2004). The processing sequence began by 'removing' all points that were not 'near' the earth based on geometric constraints used to evaluate multi-return points. The

resulting bare earth (ground) model was visually inspected and additional ground point modeling was performed in site-specific areas to improve ground detail. This manual editing of ground often occurs in areas with known ground modeling deficiencies, such as: bedrock outcrops, cliffs, deeply incised stream banks, and dense vegetation. In some cases, automated ground point classification erroneously included known vegetation (i.e., understory, low/dense shrubs, etc.). These points were manually reclassified as default. Ground surface rasters were then developed from triangulated irregular networks (TINs) of ground points.

## 4. LiDAR Accuracy Assessment

### 4.1 Laser Noise and Relative Accuracy

Laser point absolute accuracy is largely a function of laser noise and relative accuracy. To minimize these contributions to absolute error, a number of noise filtering and calibration procedures were performed prior to evaluating absolute accuracy.

#### *Laser Noise*

For any given target, laser noise is the breadth of the data cloud per laser return (i.e., last, first, etc.). Lower intensity surfaces (roads, rooftops, still/calm water) experience higher laser noise.

#### *Relative Accuracy*

Relative accuracy refers to the internal consistency of the data set - the ability to place a laser point in the same location over multiple flight lines, GPS conditions, and aircraft attitudes. Affected by system attitude offsets, scale, and GPS/IMU drift, internal consistency is measured as the divergence between points from different flight lines within an overlapping area. Divergence is most apparent when flight lines are opposing. When the LiDAR system is well calibrated, the line-to-line divergence is low (<10 cm). See Appendix A for further information on sources of error and operational measures that can be taken to improve relative accuracy.

#### **Relative Accuracy Calibration Methodology**

1. **Manual System Calibration:** Calibration procedures for each mission require solving geometric relationships that relate measured swath-to-swath deviations to misalignments of system attitude parameters. Corrected scale, pitch, roll and heading offsets were calculated and applied to resolve misalignments. The raw divergence between lines was computed after the manual calibration was completed and reported for each survey area.
2. **Automated Attitude Calibration:** All data were tested and calibrated using TerraMatch automated sampling routines. Ground points were classified for each individual flight line and used for line-to-line testing. System misalignment offsets (pitch, roll and heading) and scale were solved for each individual mission and applied to respective mission datasets. The data from each mission were then blended when imported together to form the entire area of interest.
3. **Automated Z Calibration:** Ground points per line were used to calculate the vertical divergence between lines caused by vertical GPS drift. Automated Z calibration was the final step employed for relative accuracy calibration.

## 4.2 Absolute Accuracy

The LiDAR quality assurance process uses the data from the real-time kinematic (RTK) ground survey conducted in the AOI. For this project a total of 4,331 RTK GPS measurements were collected on hard surfaces distributed among multiple flight swaths. To assess absolute accuracy the location coordinates of these known RTK ground points were compared to those calculated for the closest ground-classified laser points.

The vertical accuracy of the LiDAR data is described as the mean and standard deviation ( $\sigma$ ) of divergence of LiDAR point coordinates from RTK ground survey point coordinates. To provide a sense of the model predictive power of the dataset, the root mean square error (RMSE) for vertical accuracy is also provided. These statistics assume the error distributions for x, y, and z are normally distributed, thus we also consider the skew and kurtosis of distributions when evaluating error statistics.

Statements of statistical accuracy apply to fixed terrestrial surfaces only and may not be applied to areas of dense vegetation or steep terrain (See Appendix A).

## 5. Study Area Results

Summary statistics for point resolution and accuracy (relative and absolute) of the Chehalis River Watershed are presented below in terms of central tendency, variation around the mean, and the spatial distribution of the data (for point resolution by tile).

### 5.1 Data Summary

*Table 2. LiDAR Resolution and Accuracy - Specifications and Achieved Values.*

	Targeted	Achieved
<b>Resolution:</b>	$\geq 8$ points/m <sup>2</sup>	10.94 points/m <sup>2</sup> (1.02 points/ft <sup>2</sup> )
<b>Vertical Accuracy (1 <math>\sigma</math>):</b>	<15 cm	2.79 cm (0.09 ft)

## 5.2 Data Density/Resolution

The average first-return density of the delivered dataset is 10.94 points per square meter (Table 2). The initial dataset, acquired to be  $\geq 8$  points per square meter, was filtered as described previously to remove spurious or inaccurate points. Additionally, some types of surfaces (i.e., dense vegetation, breaks in terrain, water, steep slopes) may return fewer pulses (delivered density) than the laser originally emitted (native density).

Ground classifications were derived from automated ground surface modeling and manual, supervised classifications where it was determined that the automated model had failed. Ground return densities will be lower in areas of dense vegetation, water, or buildings.

Figures 5 and 6 show the distribution of average native and ground point densities for each delivery tile.

Cumulative LiDAR data resolution for the Chehalis River Watershed AOI:

- Average Point (First Return) Density = 1.02 points/ft<sup>2</sup> (10.94 points/m<sup>2</sup>)
- Average Ground Point Density = 0.35 points/ft<sup>2</sup> (3.75points/m<sup>2</sup>)

*Figure 3. Density distribution for first return laser points.*

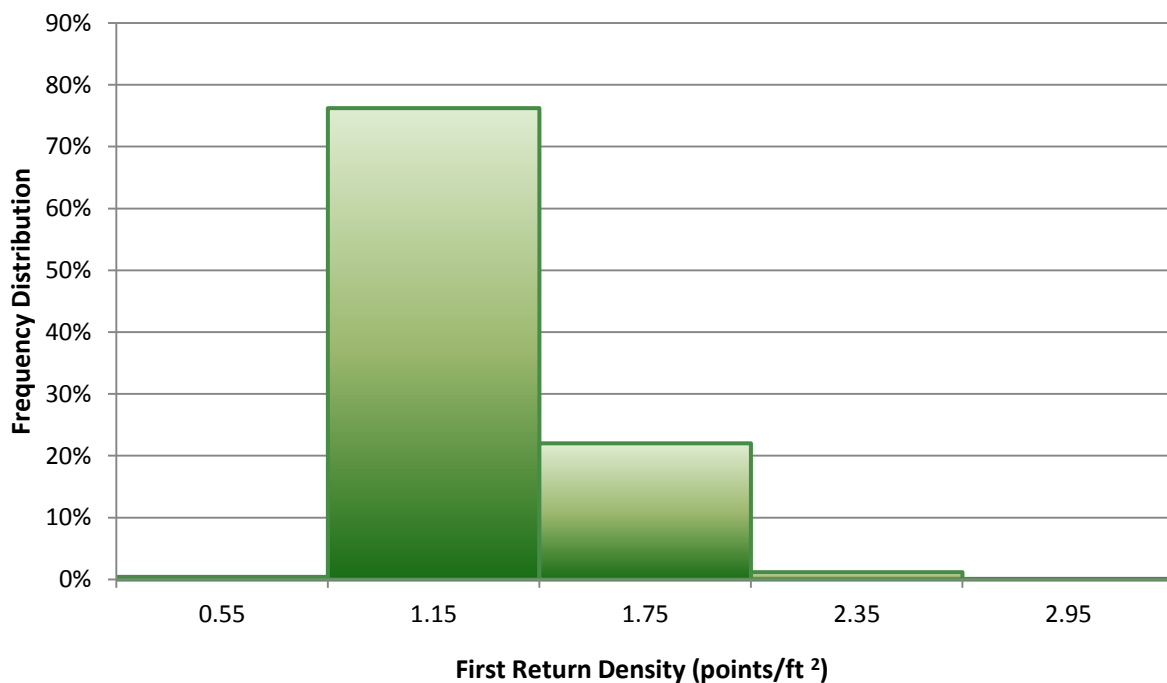




Figure 4. Density distribution for ground classified laser points.

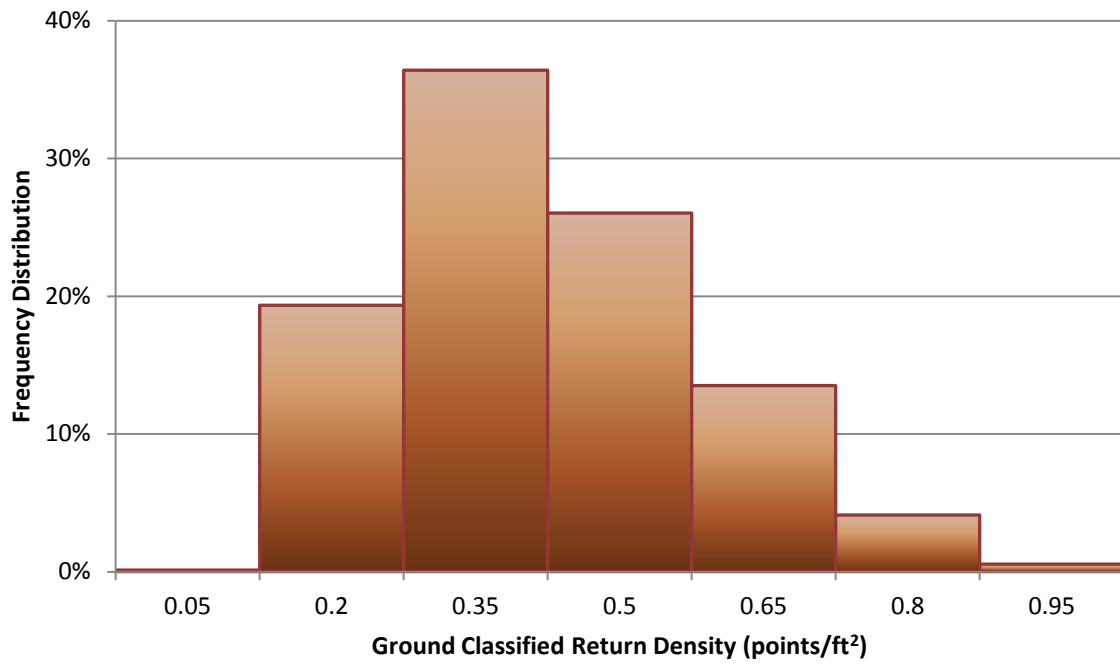
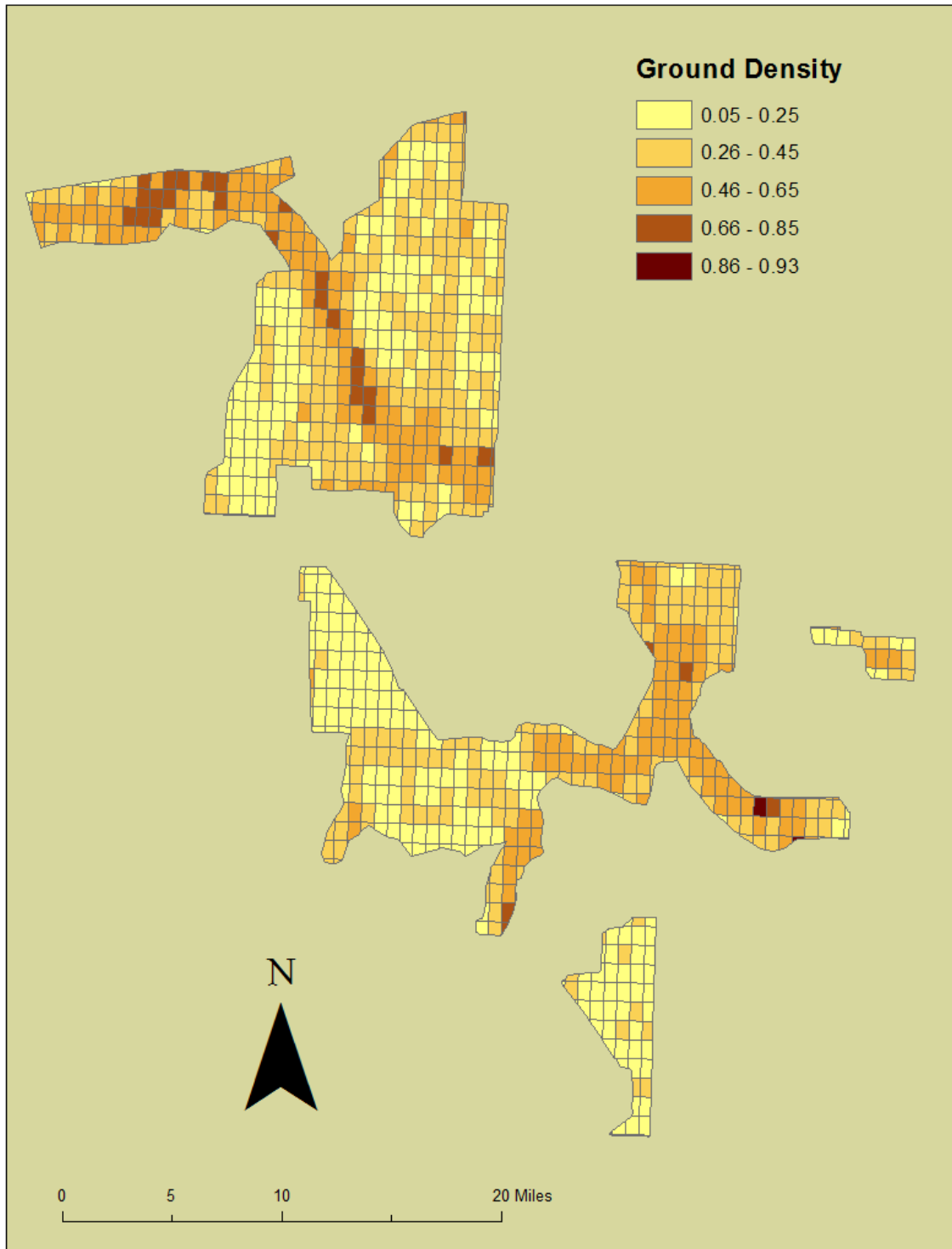


Figure 5. First Return density by 1/100<sup>th</sup> USGS tile (points/ft<sup>2</sup>).



Figure 6. Ground density by 1/100<sup>th</sup> USGS tile (points/ft<sup>2</sup>).

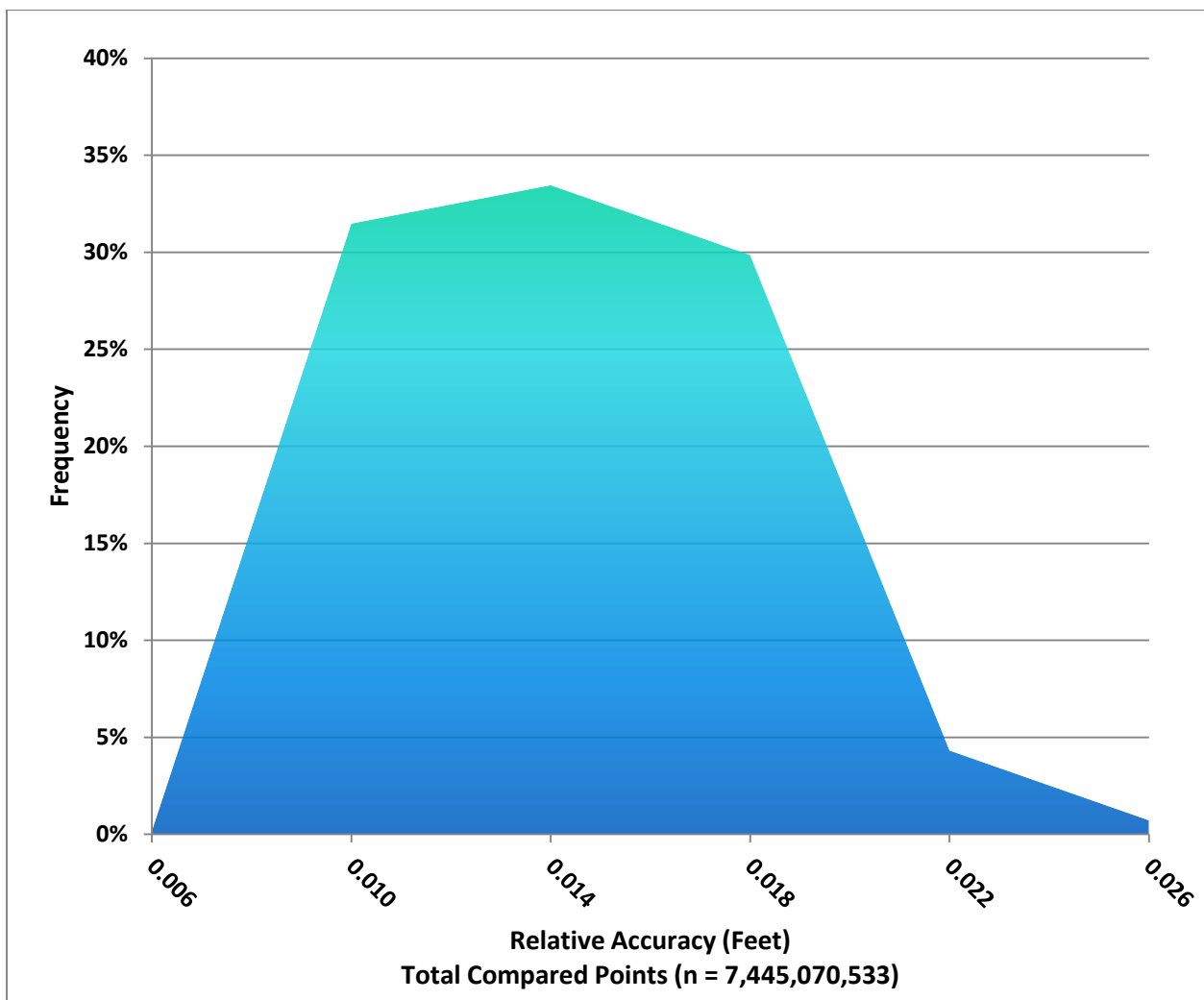


### 5.3 Relative Accuracy Calibration Results

Relative accuracy statistics for the Chehalis River Watershed AOI dataset measure the full survey calibration including areas outside the delivered boundary:

- Project Average = 0.012 ft (0.038 m)
- Median Relative Accuracy = 0.012 ft (0.039 m)
- $1\sigma$  Relative Accuracy = 0.003 ft (0.011 m)
- $1.96\sigma$  Relative Accuracy = 0.007 ft (0.022 m)
- Root Mean Square Error (RMSE) = .013 ft (.124 m)

Figure 7. Distribution of relative accuracies per flight line, non slope-adjusted.



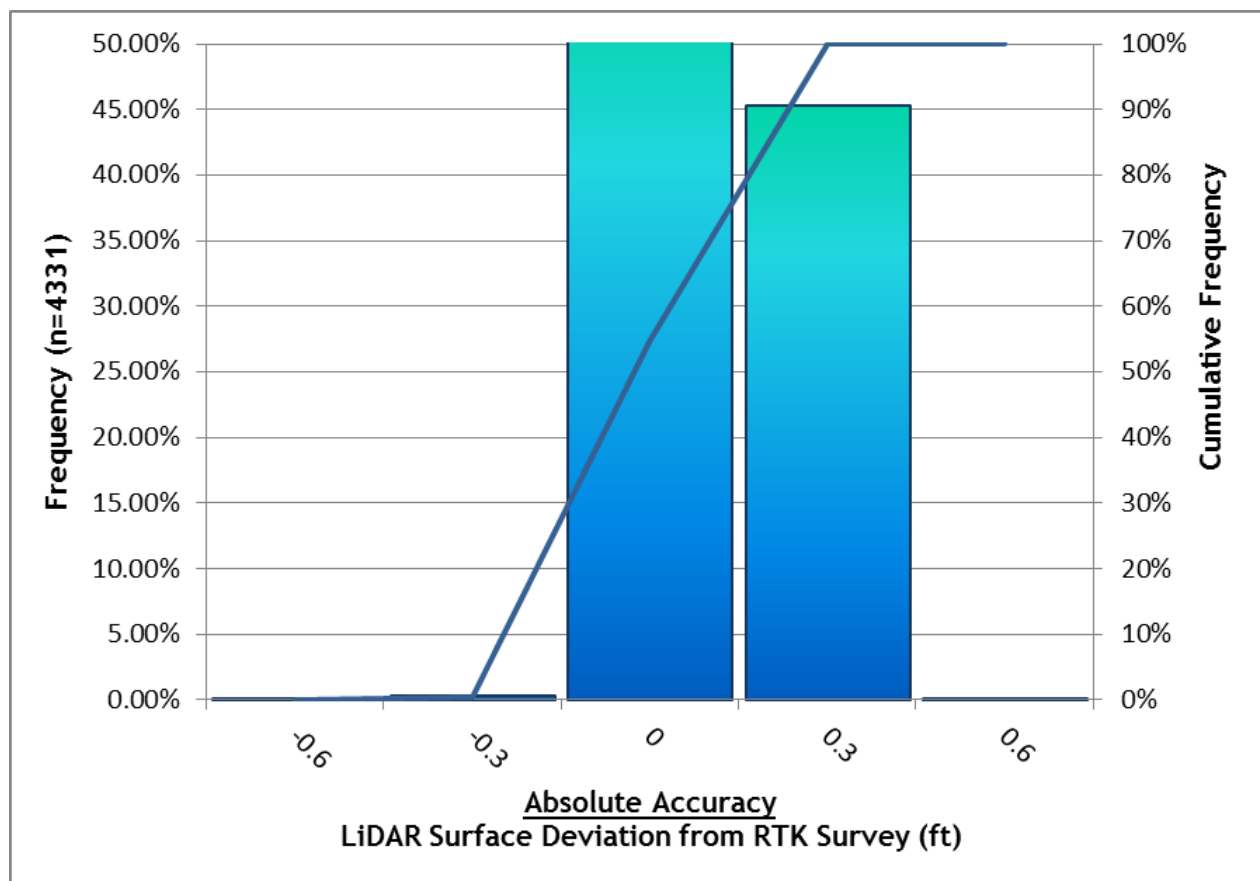
## 5.4 Absolute Accuracy

Absolute accuracies for the Chehalis River Watershed study area:

**Table 3.** Absolute Accuracy - Deviation between laser points and RTK hard surface survey points.

RTK Survey Sample Size (n): 4331		
Root Mean Square Error = 0.092 ft (.028 m)		Minimum $\Delta z$ = -0.610 ft (-0.186 m)
Standard Deviations 1 sigma ( $\sigma$ ): 0.091 ft (0.028 m)      1.96 sigma ( $\sigma$ ): 0.179 ft (0.055 m)		Maximum $\Delta z$ = 0.305 ft (0.093 m)
		Average $\Delta z$ = -0.010 ft (-0.003 m)

**Figure 8.** Absolute Accuracy - Histogram Statistics.



## 5.5 Land Cover Accuracy

Cumulative accuracies for different land cover classes collected for the Chehalis River dataset:

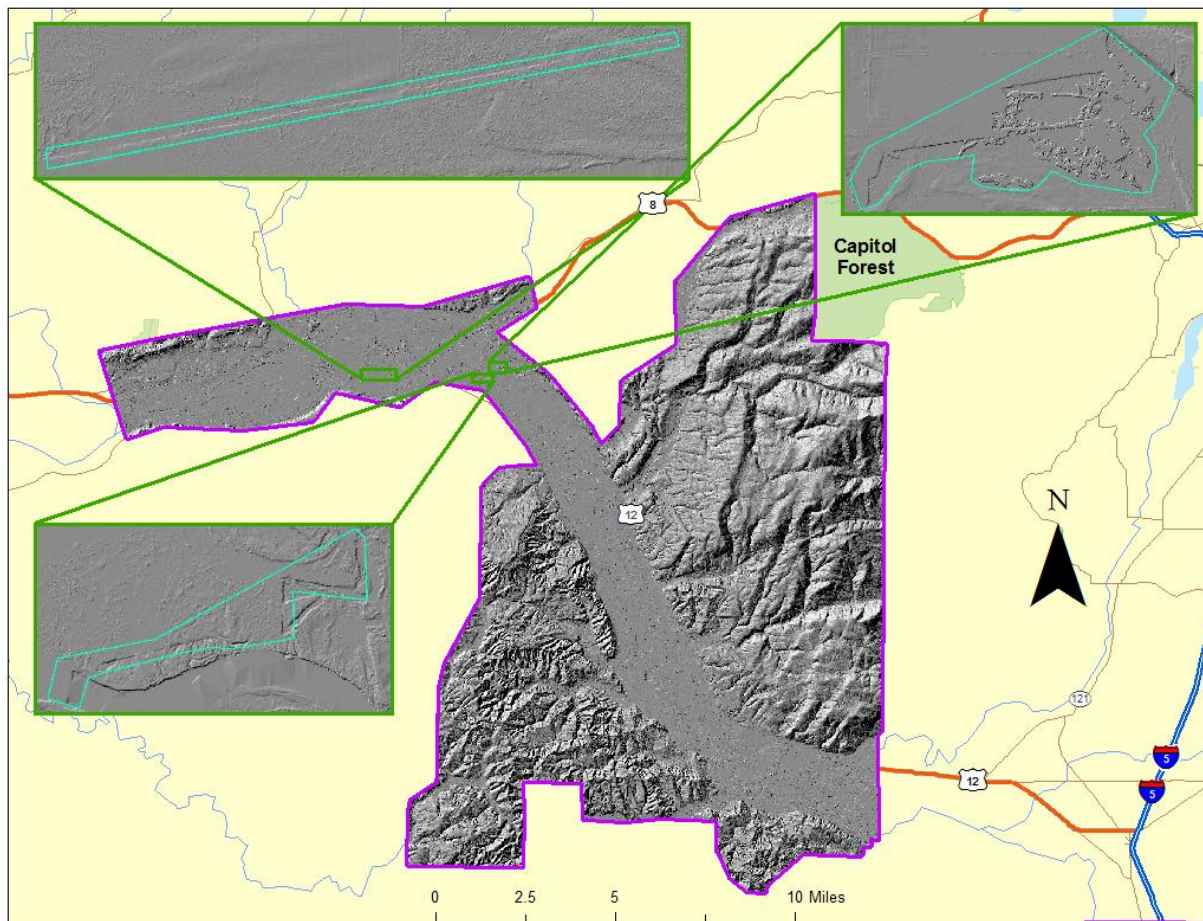
*Table 4. Land Cover Accuracy - Cumulative deviation between laser points and cover class point locations.*

Landcover Type	Count	Average (ft/m)	RMSE (ft/m)	1 Sigma (ft/m)	1.96 Sigma (ft/m)
Trees	45	0.173 ft (0.053 m)	0.249 ft (0.076 m)	0.181 ft (0.055 m)	0.355 ft (0.108 m)
Shrubs	38	0.377 ft (0.115 m)	0.437 m (0.133 ft)	0.225 m (0.069 ft)	0.442 m (0.135 ft)
Tall Grass	29	0.404 m (0.123 ft)	0.446 m (0.136 ft)	0.193 m (0.059 ft)	0.378 m (0.115 ft)
Short Grass	30	0.176 ft (0.054 m)	0.203 ft (0.062 m)	0.102 ft (0.031 m)	0.201 ft (0.061 m)

## 6. Temporal Variations

The LiDAR data collection occurred over multiple acquisition windows from January 2012 to April 2012. Acquisition days were not consecutive due to weather. Snow melt and rainfall patterns throughout these flight windows resulted in LiDAR coverage at differing water levels within the northern most part of the study area on the Chehalis River and in agricultural fields. Such differences across acquisition dates manifested in delivered data with a small 'stair step' artifact over open water (**Figure 9** ground model examples).

*Figure 9. Temporal features in the Chehalis dataset*



## 7. Hydro Flattened Models

WSI created hydro flattening breaklines for a FEMA specified portion of the North Chehalis AOI to flatten lakes and rivers greater than ~100 feet in width. The water's edge was detected using an algorithm which weights LiDAR-derived slopes, intensities, and return densities to detect the water's edge. Elevations were assigned to the water edge through neighborhood statistics identifying the lowest LiDAR return from the water surface. Lakes were assigned a consistent elevation for entire polygon while rivers were assigned consistent elevations on opposing banks and smoothed to ensure downstream flow through the entire river channel. These breaklines were incorporated into the hydro flattened DEM by enforcing triangle edges (adjacent to the breakline) to the elevation values derived from the breakline. This implementation corrected interpolation along the hard edge. Water surfaces were obtained from a TIN of the 3-D water edge breaklines resulting in the final hydroflattened model.

The rainfall and snowmelt patterns affecting the acquisition timeline (Section 6) resulted in flooding in many parts of the hydroflattened area. Due to this flooding temporary water bodies were scattered throughout the landscape. Hydroflattening is normally used to flatten only permanent water features. However, due to few to no LiDAR returns off of the temporary water bodies (mainly in agricultural fields) Watershed Sciences has flattened selected portions of temporary water bodies in areas where larger triangles and hence more interpolation was evident in the model. (Figure 10) This resulted in more consistent elevations across the temporary water bodies and eliminated the interpolation between temporary water edges.

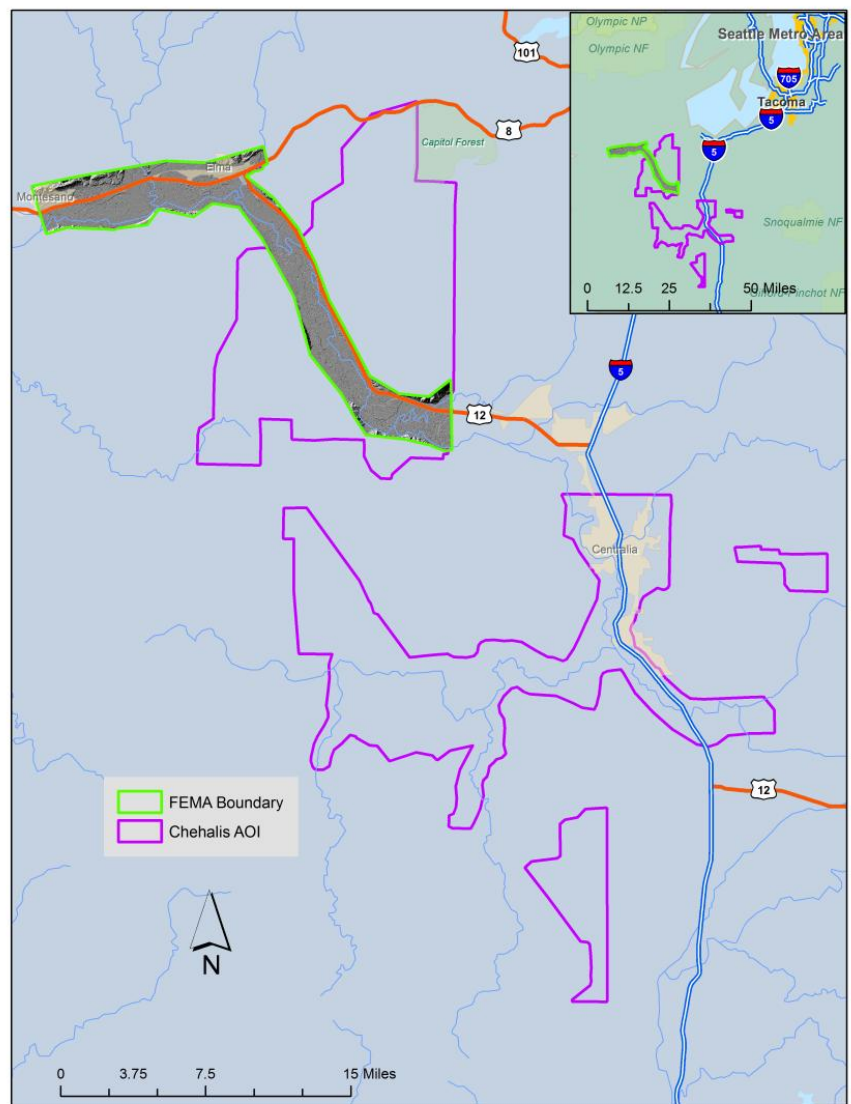
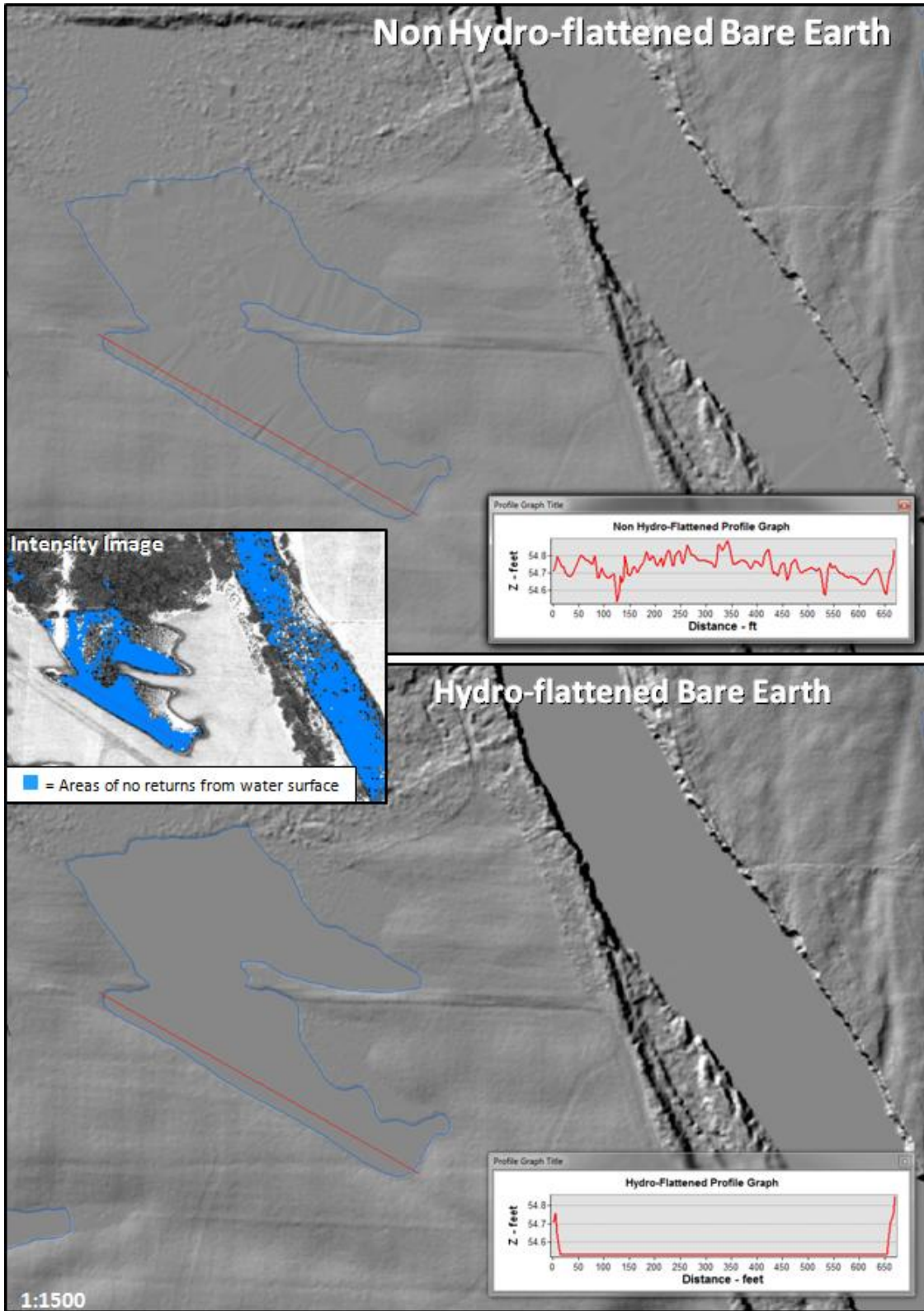




Figure 10. Hydroflattening of temporal and permanent water bodies



## 8. Projection/Datum and Units

	<b>Projection:</b>	Washington State Plane South (FIPS 4602)
<b>Datum</b>	<b>Vertical:</b>	NAVD88 Geoid03
	<b>Horizontal:</b>	NAD83 (1991 HARN)
	<b>Units:</b>	US Survey Foot

## 9. Deliverables

<b>Point Data:</b>	<ul style="list-style-type: none"> <li>• LAS 1.2 format (1/100<sup>th</sup> USGS quadrangle delineation):             <ul style="list-style-type: none"> <li>• All Returns</li> </ul> </li> <li>• ASCII text format (1/100<sup>th</sup> USGS quadrangle delineation):             <ul style="list-style-type: none"> <li>• All Returns</li> <li>• Ground points</li> </ul> </li> </ul>
<b>Vector Data:</b>	<ul style="list-style-type: none"> <li>• Tile Index for LiDAR Points (ESRI shapefile format)</li> <li>• Tile Index for Intensities (ESRI shapefile format)</li> <li>• Tile Index for Rasters (ESRI shapefile format)</li> <li>• Total Area Flown (ESRI shapefile format)</li> <li>• SBETs (ASCII text format)</li> </ul>
<b>Raster Data:</b>	<ul style="list-style-type: none"> <li>• Digital Elevation Models (ESRI GRID format, 3ft resolution, 1/4<sup>th</sup> USGS quadrangle delineation):             <ul style="list-style-type: none"> <li>• Bare Earth Model</li> <li>• Bare Earth Model Hydroflattened (FEMA AOI)</li> <li>• Highest-Hit Model</li> </ul> </li> <li>• Intensity Images (GeoTIFF format, 1.5ft resolution, 1/100<sup>th</sup> USGS quadrangle delineation)</li> </ul>
<b>Data Report:</b>	<ul style="list-style-type: none"> <li>• Full report containing introduction, methodology, and accuracy</li> </ul>

## Point Data (per 1/100th USGS Quadrangle delineation)

- LAS v1.2 or ASCII Format

\*Note: Delineation based on 1/100<sup>th</sup> of a full 7.5-minute USGS Quadrangle (0.75-minutes). Larger delineations, such as 1/4<sup>th</sup> USGS Quadrangles, resulted in unmanageable file sizes due to high data density.

Figure 10. Quadrangle naming convention for 1/100th of a 7.5-minute USGS Quad.



## 10. Certifications

Watershed Sciences provided LiDAR services for the Chehalis River Watershed study area as described in this report.

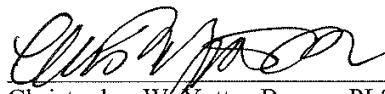
I, Russ Faux, have reviewed the attached report for completeness and hereby state that it is a complete and accurate report of this project.



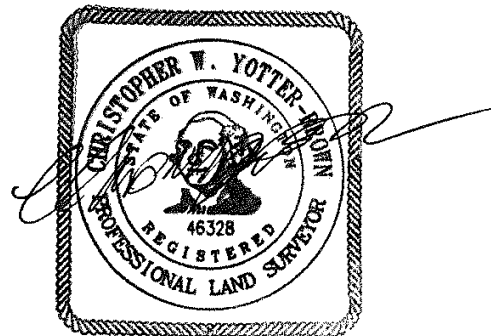
---

Russ Faux  
Principal  
Watershed Sciences, Inc.

I, Christopher W. Yotter-Brown, being first dully sworn, say that as described in the Ground Survey subsection of the Acquisition section of this report was completed by me or under my direct supervision and was completed using commonly accepted standard practices. Accuracy statistics shown in the Accuracy Section have been reviewed by me to meet National Standard for Spatial Data Accuracy.



6/21/2012  
Christopher W. Yotter-Brown, PLS Oregon & Washington  
Watershed Sciences, Inc  
Portland, OR 97204



Renews: 12/21/2012

---

LiDAR Data Acquisition and Processing: Chehalis River Watershed Study Area

Prepared by Watershed Sciences, Inc.

# 11. Selected Images

*Figure 11. View looking northwest at a quarry west of Packwood Creek, WA. The image is a 3D point cloud colored by height and intensity.*

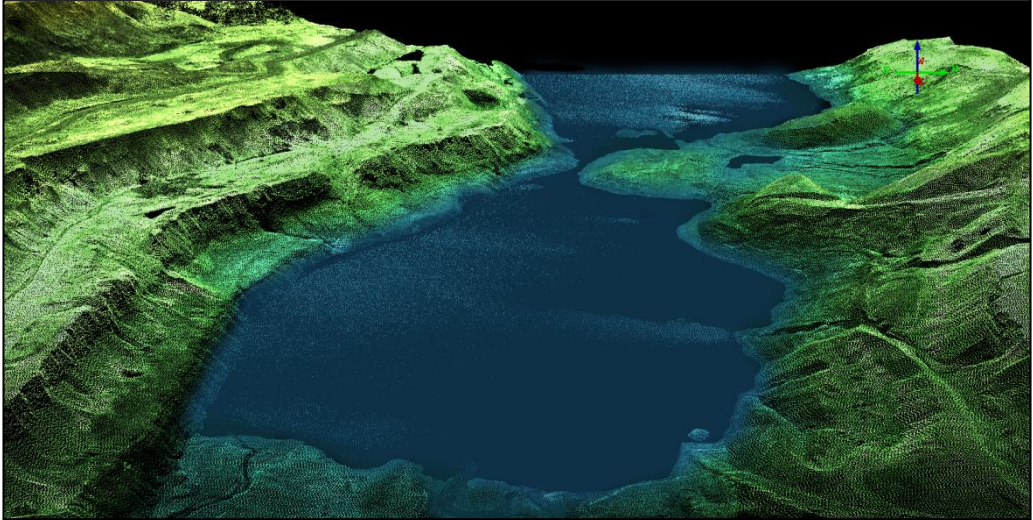


*Figure 12. View looking east toward Packwood Creek, WA at two cranes. The image is a 3D point cloud colored by height and intensity.*

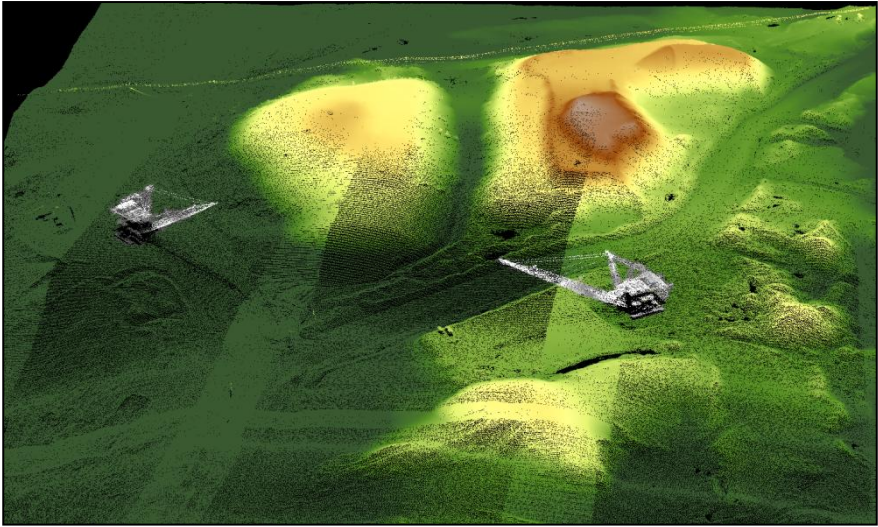


**Figure 13.** 3D highest hit model looking north at the highway 6/4<sup>th</sup> Avenue Bridge crossing the Chehalis River in Pe Ell, WA.

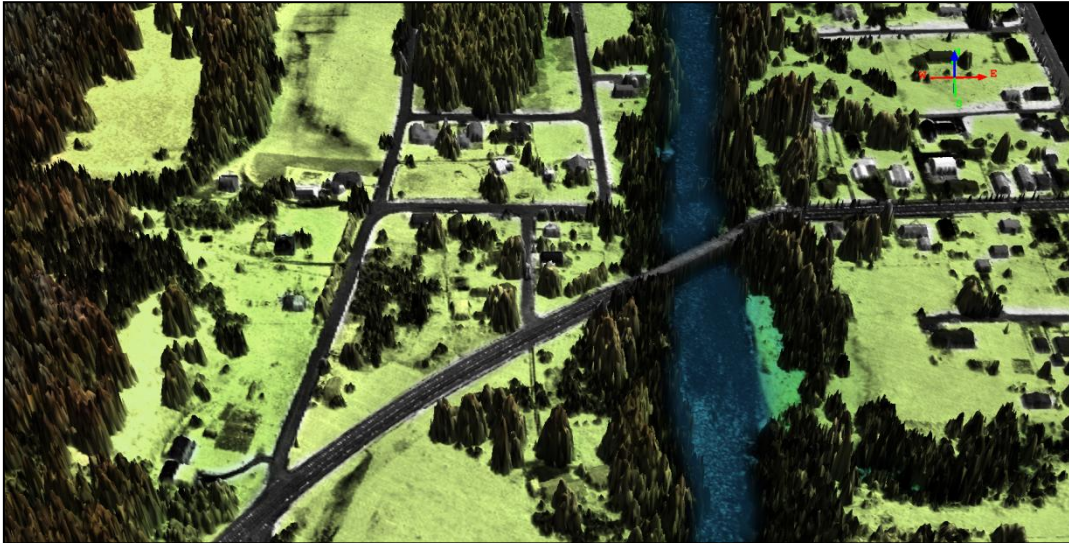


**Figure 14.** 3D point cloud model looking north at the highway 6/4<sup>th</sup> Avenue Bridge crossing the Chehalis River in Pe Ell, WA.

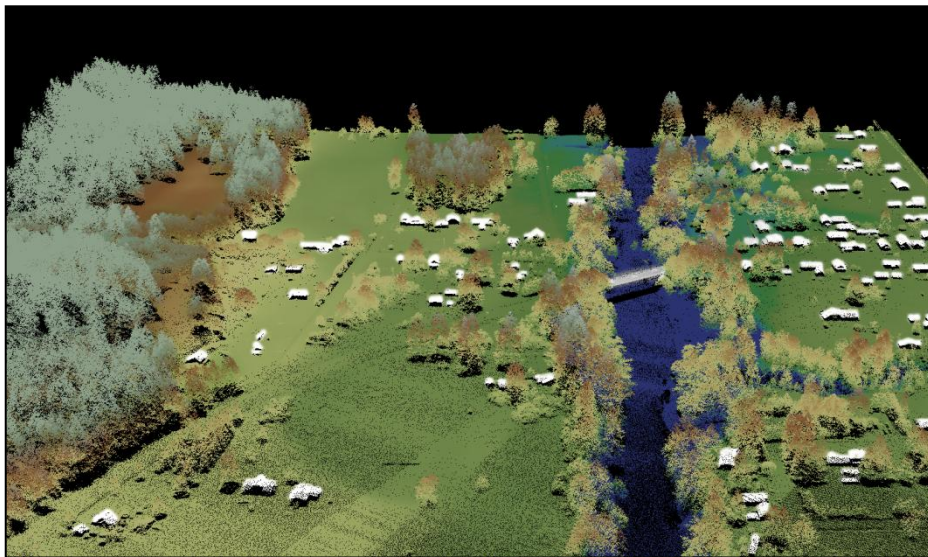
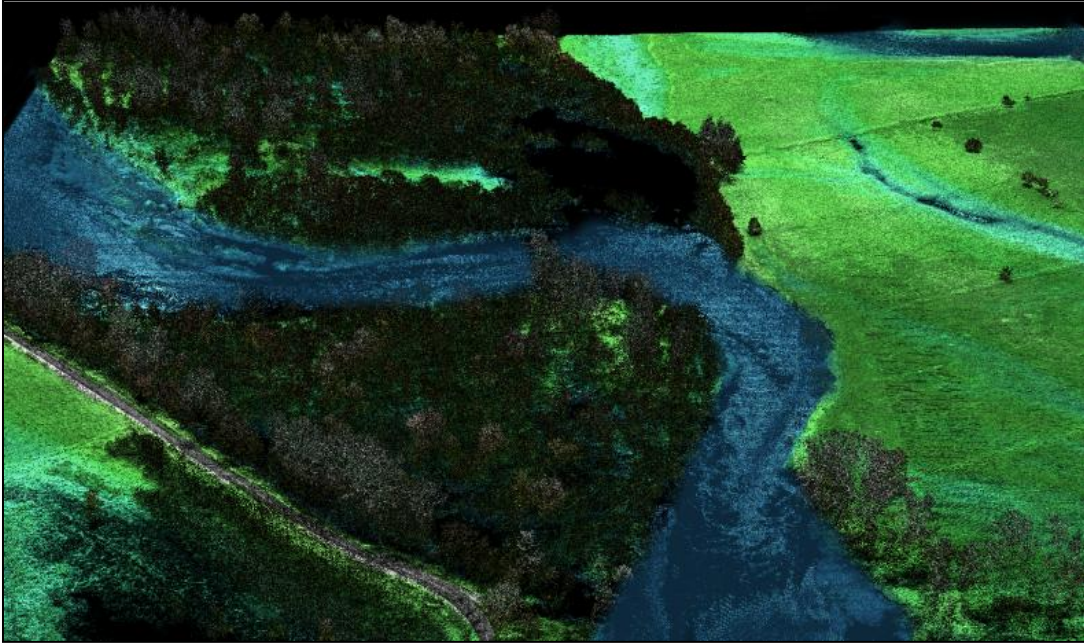


**Figure 15.** View south along the Chehalis River, WA where Elma Gate Rd follows the river east of highway 12. The image is a 3D point cloud model.



## 12. Glossary

**1-sigma ( $\sigma$ ) Absolute Deviation:** Value for which the data are within one standard deviation (approximately 68<sup>th</sup> percentile) of a normally distributed data set.

**1.96-sigma ( $\sigma$ ) Absolute Deviation:** Value for which the data are within two standard deviations (approximately 95<sup>th</sup> percentile) of a normally distributed data set.

**Root Mean Square Error (RMSE):** A statistic used to approximate the difference between real-world points and the LiDAR points. It is calculated by squaring all the values, then taking the average of the squares and taking the square root of the average.

**Pulse Rate (PR):** The rate at which laser pulses are emitted from the sensor; typically measured as thousands of pulses per second (kHz).

**Pulse Returns:** For every laser pulse emitted, the Leica ALS 50 Phase II system can record *up to four* wave forms reflected back to the sensor. Portions of the wave form that return earliest are the highest element in multi-tiered surfaces such as vegetation. Portions of the wave form that return last are the lowest element in multi-tiered surfaces.

**Accuracy:** The statistical comparison between known (surveyed) points and laser points. Typically measured as the standard deviation (sigma,  $\sigma$ ) and root mean square error (RMSE).

**Intensity Values:** The peak power ratio of the laser return to the emitted laser. It is a function of surface reflectivity.

**Data Density:** A common measure of LiDAR resolution, measured as points per square meter.

**Spot Spacing:** Also a measure of LiDAR resolution, measured as the average distance between laser points.

**Nadir:** A single point or locus of points on the surface of the earth directly below a sensor as it progresses along its flight line.

**Scan Angle:** The angle from nadir to the edge of the scan, measured in degrees. Laser point accuracy typically decreases as scan angles increase.

**Overlap:** The area shared between flight lines, typically measured in percents; 100% overlap is essential to ensure complete coverage and reduce laser shadows.

**DTM / DEM:** These often-interchanged terms refer to models made from laser points. The digital elevation model (DEM) refers to all surfaces, including bare ground and vegetation, while the digital terrain model (DTM) refers only to those points classified as ground.

**Real-Time Kinematic (RTK) Survey:** GPS surveying is conducted with a GPS base station deployed over a known monument with a radio connection to a GPS rover. Both the base station and rover receive differential GPS data and the baseline correction is solved between the two. This type of ground survey is accurate to 1.5 cm or less.



## 13. Citations

Soininen, A. 2004. TerraScan User's Guide. TerraSolid.

## Appendix A

### LiDAR accuracy error sources and solutions:

Type of Error	Source	Post Processing Solution
GPS (Static/Kinematic)	Long Base Lines	None
	Poor Satellite Constellation	None
	Poor Antenna Visibility	Reduce Visibility Mask
Relative Accuracy	Poor System Calibration	Recalibrate IMU and sensor offsets/settings
	Inaccurate System	None
Laser Noise	Poor Laser Timing	None
	Poor Laser Reception	None
	Poor Laser Power	None
	Irregular Laser Shape	None

### Operational measures taken to improve relative accuracy:

1. Low Flight Altitude: Terrain following is employed to maintain a constant above ground level (AGL). Laser horizontal errors are a function of flight altitude above ground (i.e., ~ 1/3000<sup>th</sup> AGL flight altitude).
2. Focus Laser Power at narrow beam footprint: A laser return must be received by the system above a power threshold to accurately record a measurement. The strength of the laser return is a function of laser emission power, laser footprint, flight altitude and the reflectivity of the target. While surface reflectivity cannot be controlled, laser power can be increased and low flight altitudes can be maintained.
3. Reduced Scan Angle: Edge-of-scan data can become inaccurate. The scan angle was reduced to a maximum of  $\pm 15^\circ$  from nadir, creating a narrow swath width and greatly reducing laser shadows from trees and buildings.
4. Quality GPS: Flights took place during optimal GPS conditions (e.g., 6 or more satellites and PDOP [Position Dilution of Precision] less than 3.0). Before each flight, the PDOP was determined for the survey day. During all flight times, a dual frequency DGPS base station recording at 1-second epochs was utilized and a maximum baseline length between the aircraft and the control points was less than 19 km (11.5 miles) at all times.
5. Ground Survey: Ground survey point accuracy (i.e. <1.5 cm RMSE) occurs during optimal PDOP ranges and targets a minimal baseline distance of 4 miles between GPS rover and base. Robust statistics are, in part, a function of sample size (n) and distribution. Ground survey RTK points are distributed to the extent possible throughout multiple flight lines and across the survey area.
6. 50% Side-Lap (100% Overlap): Overlapping areas are optimized for relative accuracy testing. Laser shadowing is minimized to help increase target acquisition from multiple scan angles. Ideally, with a 50% side-lap, the most nadir portion of one flight line coincides with the edge (least nadir) portion of overlapping flight lines. A minimum of 50% side-lap with terrain-followed acquisition prevents data gaps.
7. Opposing Flight Lines: All overlapping flight lines are opposing. Pitch, roll and heading errors are amplified by a factor of two relative to the adjacent flight line(s), making misalignments easier to detect and resolve.